Biomed Microdevices (2009) 11:883–892
DOI 10.1007/s10544-009-9305-9

Microdevice for the isolation and enumeration of cancer cells from blood

Swee Jin Tan · Levent Yobas · Gabriel Yew Hoe Lee · Choon Nam Ong · Chwee Teck Lim

Published online: 23 April 2009
© Springer Science + Business Media, LLC 2009

Abstract Cancer metastasis is the main attribute to cancer-related deaths. Furthermore, clinical reports have shown a strong correlation between the disease development and number of circulating tumor cells (CTCs) in the peripheral blood of cancer patients. Here, we present a label-free microdevice capable of isolating cancer cells from whole blood via their distinctively different physical properties such as deformability and size. The isolation efficiency is at least 80% for tests performed on breast and colon cancer cells. Viable isolated cells are also obtained which may give further insights to the understanding of the metastatic process. Contrasting with conventional biochemical techniques, the uniqueness of this microdevice lies in the mechanistic and efficient means of isolating viable cancer cells in blood. The microdevice has the potential to be used for routine monitoring of cancer development and cancer therapy in a clinical setting.

Keywords Circulating tumor cells (CTCs) · Microfluidic device · Cancer cell isolation · Metastasis · Physical separation · Biomechanical properties · Cell mechanics

Electronic supplementary material The online version of this article (doi:10.1007/s10544-009-9305-9) contains supplementary material, which is available to authorized users.

S. J. Tan · L. Yobas
Institute of Microelectronics,
A*STAR (Agency for Science, Technology and Research),
11 Science Park Road, Singapore Science Park II,
Singapore 117685, Singapore

S. J. Tan · C. T. Lim
Graduate School for Integrative Sciences and Engineering,
National University of Singapore,
12 Medical Drive,
Singapore 117598, Singapore

G. Y. H. Lee · C. T. Lim
Singapore-MIT Alliance,
4 Engineering Drive 3,
Singapore 117576, Singapore

C. N. Ong
Department of Epidemiology and Public Health,
National University of Singapore,
16 Medical Drive,
Singapore 117597, Singapore

C. T. Lim (✉)
Division of Bioengineering and Department of Mechanical Engineering, National University of Singapore,
9 Engineering Drive 1,
Singapore 117576, Singapore
e-mail: ctlim@nus.edu.sg

1 Introduction

Isolation and enumeration of circulating tumor cells (CTCs) in peripheral blood has clinical significance in combating cancer (Reuben et al. 2008; Urtishak et al. 2008). Deaths resulting from cancer are mainly due to late diagnosis of the disease and when metastasis has occurred (Gupta and Massague 2006; Steeg 2006). To ensure patients receive timely treatment, enumerating CTCs in blood can complement existing early detection methods. Furthermore, blood samples being a routinely extracted body fluid in any health test can be easily obtained to check for CTCs. CTCs are found in patients with metastatic carcinomas (Allard et al. 2004; Steen et al. 2008) and are associated with the disease progression (Cristofanilli et al. 2004; Mocellin et al. 2006; Wiedswang and Naume 2007). The effectiveness of therapeutic treatments can also be measured by the number of CTCs in blood (Nole et al. 2007; Rolle et al. 2005). Thus, there is

much interest in isolating, quantifying and studying these cells obtained from peripheral blood.

CTCs are of very low concentration in blood which poses the technical difficulty to detect these rare cells (Losanoff et al. 2008; Zieglschmid et al. 2005). The absolute number of CTCs in blood of cancer patients varies and depends on the conditions of the patients. Leading techniques to enumerate CTCs include immuno-magnetic separation followed by immunocytochemistry detection (Cristofanilli et al. 2004; Yagata et al. 2008) and RT-PCR to indicate the presence of CTCs in peripheral blood (Mattano et al. 1992; Schroder et al. 2003). These methods have been successfully demonstrated on various cancer types (Dawood et al. 2008; Szatanek et al. 2008; Wong et al. 2008). Alternative methodologies such as a direct visualization assay (Kahn et al. 2004), fluorescent activated cell sorter (FACS) (Moreno et al. 2001), fibre-optic array scanning technology (FAST) cytometer (Krivacic et al. 2004) and anti-EpCAM coated microfabricated structures (Nagrath et al. 2007) have also been used to enumerate CTCs in blood samples. Complex procedures, tedious inspections and long processing time are the limiting factors associated with most existing techniques. Furthermore, viability of the isolated cells are lost as fixing of the samples is required by most existing techniques. There is much to understand about the condition of CTCs whilst in circulation (Pantel et al. 2008) and having viable cells after isolation will allow studies to be carried out on CTC sub-populations. This may provide valuable insights to the biological characteristics of the disease such as the link between cancer stem cells and metastasis. Although a recent study has successfully isolated viable CTCs (Nagrath et al. 2007), the isolated cells may be difficult to retrieve due to the bindings of the tumor associated antigens to the device. Retrieving these cells may require high mechanical forces or biochemical agents and the integrity of these cells might be affected as a result (Chang et al. 2008). In addition, most methodologies will require functional modifications which is less desirable (Lara et al. 2004).

Microfluidic devices provide an alternative technique compared to conventional biochemical separations. Devices utilizing dielectrophoretic forces to separate and manipulate cells are advantageous as they do not require functionalization of the sample or the microdevice (Chiou et al. 2005; Gray et al. 2004; Rosenthal and Voldman 2005; Voldman 2006). However, efficient cancer cell separation may be difficult due to the low concentration of CTCs in blood and the relative similar dimensions of leukocytes with cancer cells. Here, we present a microfluidic device to isolate viable cancer cells of breast and colon origins from whole blood using solely the biorheological property differences of cancer cells and blood constituents. No functional modifications of the microdevice are required as isolation is solely dependent on the biorheological property differences of cancer cells and blood constituents. Past studies have revealed that the shear modulus, stiffness, size and deformability of cancer cells (Weiss 1990; Weiss and Dimitrov 1986) is distinctively different from blood constituents (Mohamed et al. 2004; Shelby et al. 2003). The adopted approach draws upon this dissimilarity to achieve the high purity in isolating cancer cells in blood. A feasibility study has also been successfully conducted to separate samples based on biorheological differences (Tan et al. 2008). The isolation process is achieved in a single step, preserving the integrity and viability of these cells. Retrieval of the isolated cells is also straightforward by controlling and manipulating the flow conditions in our device.

2 Materials and methods

2.1 Microdevice design and fabrication

Figure 1 shows the experimental setup and the design of the microdevice. Multiple arrays of crescent-shaped isolation wells are created in the microchannel to isolate cancer cells while allowing blood constituents to sieve through (Fig. 1b). The gaps of 5 μm in each of the traps ensure the exit of blood constituents due to their ability to traverse very small constrictions (Fig. 1c). In this way, larger white blood cells (WBCs) of comparable dimensions to but more deformable than cancer cells can be effectively removed and this will ensure a high purity of trapped cancer cells. Each trap is positioned with pitch of 50 μm which effectively prevents cells from clogging in the microdevice. The pre-filters with gaps of 20 μm shown in Fig. 1(c) also serve to prevent larger clumps or debris from clogging up the setup and are connected to the waste outlet to effectively remove debris. Clogging prevention is important to achieve a feasible device and maximizing isolation purity is required to reduce false positive results which are likely encountered problems by devices that try to separate and isolate cells through physical means (Di Carlo et al. 2006; Mohamed et al. 2004; Pamme 2007). In addition, each layer of isolation structures is offset by 25 μm to enhance hydrodynamic efficiency (Fig. 1c). The isolation traps are further divided into two sections that facilitated maximal retrieval of isolated cells. During cell retrieval, the flow direction is reversed from the indicated arrows shown in Fig. 1(b) and the rounded inverted crescent-shaped structures provided a favourable path to enable the cells to be extracted out to the cell collection point. It also minimizes physical interactions to reduce possible mechanical damage to cells during retrieval. For each microdevice, there are a total of 900 isolation structures.

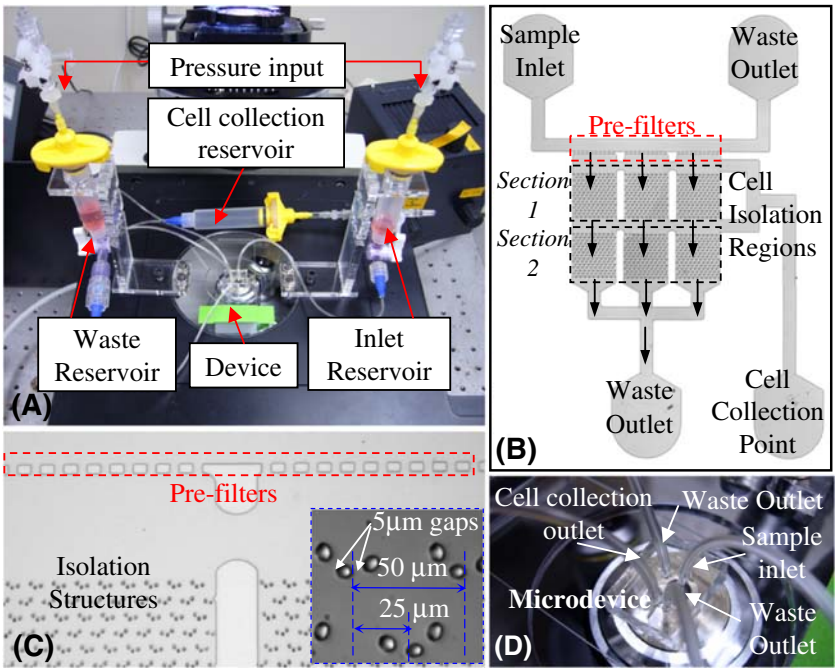

Fig. 1 Microdevice for cancer cell isolation and enumeration. (**a**) Custom made experimental setup mounted on the inverted microscope. (**b**) Microdevice layout. (**c**) Enlarged view of pre-filters and arrays of cell isolation wells. Pre-filters with gaps of width 20 µm and are used to prevent cell clumps from entering. Isolation layers are offset by 25 µm to enhance trapping efficiency. (**d**) Fluidic connections to microdevice

The arrays of crescent-shaped structures are created using soft lithography (McDonald and Whitesides 2002). The photo mask is drawn in Cadence (Cadence Design Systems, Inc., San Jose, CA, USA) and produced on glass with critical dimensions of 2 µm (Infinite Graphics Inc., Minneapolis, MN, USA). Fabrication of the masters are done by spin coating (3,200 rpm, 45 s) SU-8 2025 (MicroChem Corp., Newton, MA, USA) on an 8-inch silicon wafer. Depth of the microdevice is 18 µm and cast from polydimethylsiloxane (PDMS) (Sylgard 184, Dow Corning Corp., Midland, MI, USA). Following manufacturer's instructions, pre-cured PDMS is degassed in a desiccator and cured in an oven preset at 80 °C for 2 h. After peeling the PDMS off the master, fluidic ports are punched using a flat tip needle. Irreversible bonding of the PDMS microdevice to a glass slide is achieved using oxygen plasma treatment.

2.2 Computational Fluids Dynamics (CFD) analysis

A 3D computational model of the microdevice is developed to better understand the flow characteristics as well as to help in the design of the microdevice. A simplified model of the microdevice consisting of fourteen isolation structures is created using Gambit (Ansys Inc., Lebanon, NH, USA) and simulated using Fluent (Ansys Inc., Lebanon, NH, USA). An optimized mesh number of 579,820 is used. Mesh independence is ascertained by increasing the mesh number and observing the difference in velocities to be less than 1%. Adopting a no-slip wall boundary condition and fluid properties of pure H_2O (density at 998.2 kg/m^3 and viscosity 0.001003 Pa.s), the study is carried out by analyzing the velocity profiles and shear stresses at the irregular isolation structures under different initial conditions.

With the computational results, simulated particles can be traced in the flow to check upon the isolation effectiveness of the microdevice. 25 simulated particles are placed uniformly at the inlet and the flow pathlines traced to check if they intercept the crescent traps. Where the pathlines intercept with the crescent trap, it is presumed that there is a possibility for cells in the sample solution to be impeded. This helps to determine if the design is able to fulfil its task effectively. When simulating in the reverse flow direction for cell retrieval, the flow pathlines of the simulated particles aid to determine if the isolation structures obstruct the recovery. This is crucial to ensure minimal damage to the isolated cells. The shear stresses and flow patterns in the microdevice at various operating conditions are extracted from the computational analysis and compared to physiological conditions to aid in optimizing the design and determining the operating conditions for the microdevice.

2.3 Cell culture and cell size measurements

Three different cell lines MCF-7, MDA-MB-231 (human adenocarcinomas) and HT-29 (human colon adenocarcinoma) of human origin are tested in the microdevice. Culturing of cells are done in a 25 cm^2 tissue culture flask and maintained with Dulbecco's Modified Eagle Medium (DMEM) (Sigma, St. Louis, MO, USA) supplement with 10% fetal bovine serum (FBS) (Hyclone, Logan, UT, USA) and 1% penicillin

G/ streptomycin/ amphotericin B (Gibco, Carlsbad, CA, USA). For each experiment, cells are grown to confluence, trypsinized and resuspended in culture media. A portion of the suspended cells are taken as control in the experiment and cultured normally. The rest are diluted to a concentration of approximately 100 cells per milliliter and the sample solution is injected into the device for characterizing its isolation efficiency. In the cell proliferation analysis, isolated cells are retrieved from the microdevice and reseeded into the culture flask to observe its proliferation status over a period of 5 days under normal culturing conditions.

For cell size measurements of the cancer cell lines, the diameter is an average reading obtained from images of 100 suspended cells and determined using an image processing software (NIS-Elements AR, Nikon Corp., Singapore). Cancer cell counting is done with a hemocytometer and serial diluted to achieve the desired concentration of 100 cells per milliliter of 1× phosphate buffered saline (PBS).

2.4 Sample and apparatus preparation

All apparatus including the microdevices, tubes and fluidic connectors, are thoroughly sterilized with 70% ethanol prior to use. Subsequently, sterile 1× PBS is injected to wash out any traces of ethanol. The microdevice is then mounted in a custom made fixture with the fluidic connections attached (Fig. 1d). The fixture allows portability of the setup and positions the sample solution close to the microdevice to minimize sample wastage. To control the flow in the microdevice, two pressure regulators are used to create the pressure differential between the inlet and the waste reservoir. The use of pressure regulation enables instantaneous and real time changes to the flow characteristics in the device.

To ascertain the isolation purity, each of the cancer cell types are added into whole blood donated from healthy donors at concentration of approximately 100 cells per milliliter. The sample solution is further diluted with sterile 1× PBS in a 1:2 ratio to reduce the sample viscosity so that it can be processed easily. Isolated cells in the microdevice are stained with fluorescence (see protocol in next section) to distinguish between cancer cells and WBCs. For cell proliferation experiments, isolated cells are retrieved by reversing the pressure differential and directing the isolated cells to the collection point. The collected solution is then centrifuged at 1,200 rpm for 5 min with the cell pellet resuspended later in culturing media DMEM and reseeded in a T25 culture flask. Their proliferative rates are compared to normal cultures which act as controls in the experiment. A further part of the analysis involves testing the microdevice at lower concentrations of cancer cells in sterile 1× PBS (1–3 cells per ml). Cells are picked out manually using a pipette with a 200 μl pipette tip from a cell suspension of approximately 100 cells per milliliter under the microscope. The cells are then directly added to 1× PBS and injected into the microdevice.

2.5 Immunofluorescence staining to identify CTCs

Immunofluorescence staining allows the visual examination to characterize cancer cell isolation purity in the microdevice. For the control experiment, the premixed sample of blood and cancer cells (200 μl) is incubated onto a 12 mm coverslip (polylysine coated) for 30 min. The sample is subsequently fixed with 4% paraformaldehyde (PFA) for 30 min and washed with 1× PBS for 15 min. It is then permeabilized by 0.1% Triton X-100 in 1× PBS for 10 min, followed by a PBS wash for 15 min and added 10% goat serum for 30 min to block out non-specific bindings. The sample is then stained for Epithelial Cell Adhesion Molecule (EpCAM) (1:50, Santa Cruz Biotechnology Inc., Santa Cruz, CA, USA) for 1 h followed by the secondary antibody (1:500, goat anti-mouse AlexaFluor 568, Invitrogen Corp., Carlsbad, CA, USA) for another hour to identify cancer cells. Fluorescein isothiocyanate (FITC) conjugated CD45 (1:50, Santa Cruz Biotechnology Inc. , Santa Cruz, CA, USA) is then used (1 h) to identify WBCs and 4',6-diamidino-2-phenylindole (DAPI) for nuclei visualization. The coverslip is then washed with 1× PBS for 10 min and mounted.

For staining in the microdevice, a pressure differential of 5 kPa is used to induce flow into the microdevice. The value of 5 kPa is chosen as it best preserves the state of the isolated cells in the microdevice as compared to using higher pressure differentials. Lower pressure conditions will increase the processing time. Captured cells are first fixed by flowing 4% PFA for 30 min, permeabilized by 0.1% Triton X-100 in 1× PBS for 10 min, followed by washing with 1× PBS for 15 min and added 10% goat serum to block out non-specific bindings for 30 min. To identify cancer cells, 0.2 ml of EpCAM antibodies are injected for 15 min, left to stand for another 45 min and followed by PBS washing. The procedures of antibody injection and PBS wash are repeated for the secondary antibody (1:500, goat anti-mouse AlexaFluor 568). For the identification of WBCs, 0.2 ml of FITC conjugated CD45 antibodies are injected for 15 min, left to stand for another 45 min and followed by washing with PBS. Staining is completed by flowing DAPI for 15 min at 5 kPa followed by washing with PBS.

3 Results and discussion

3.1 Clinical significance and CFD analysis

The prognostic values of enumerating CTCs in peripheral blood have been widely reported (Beitsch and Clifford

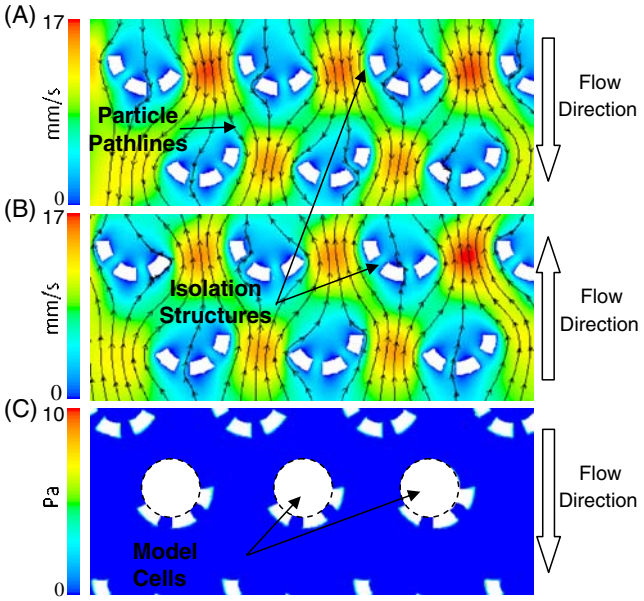

Fig. 2 Computational analysis of the flow and shear stress around the isolation wells at the operating pressure of 5 kPa. (**a**) Velocity profile when isolating cells taken at mid-plane (10 μm from the base) of the model. (**b**) Velocity profile when retrieving cells. (**c**) Shear stress acting on a spherical cell model when the cells are arrested in the isolation structures

2000; Budd et al. 2006; Cristofanilli et al. 2007; Gogas et al. 2002; Hayes et al. 2006; Hoon 2004). This method is also minimally invasive as compared to traditional biopsies. The number of CTCs in blood is directly associated with the disease progression and can help in evaluating cancer treatment efficacy (Nole et al. 2007). Thus, it is important to have a high cancer cell isolation efficiency for the microdevice to count these rare cells in blood samples accurately. Our approach draws mainly upon the highly deformable nature of erythrocytes (Shelby et al. 2003) and leukocytes (Yap and Kamm 2005) that enable these cells to traverse capillaries as small as 2–5 μm whose cell diameters can range from 8 to 25 μm. On the other hand, cancer cells are more likely to be arrested in capillaries of similar dimensions (Weiss and Dimitrov 1984). Average sizes of MCF-7, MDA-MB-231 and HT-29 cells used in the experiments are tabulated to be 16.2 ± 1.80 μm, 17.9 ± 2.94 μm and 15.5 ± 1.25 μm respectively.

In order to understand the flow profile around the irregular shaped structures and ascertain minimal damage on isolated cancer cells due to hydrodynamic forces, the fluid velocity and shear stress profiles are simulated for the operating pressure differentials applied. Figure 2 depicts the velocity patterns and flow path surrounding the isolation structures at the operating pressure of 5 kPa. In isolating cancer cells (Fig. 2a), the gaps facilitate the entry of the cells as shown by the traced path lines of the simulated particles. Flow velocities are also much lower near the isolation regions. In addition, the flow path is diverted when the trap is occupied which prevents clogging. The crescent shape of the isolation well which is alternated left and right aid to prevent clogging as well and allow each isolation well to hold a single cell. Due to the heterogeneous nature of the cell sample, the cell sizes have a relatively significant variation. Traps occupied by smaller cells tend to be able to hold more than one cell. With this design, it helps to divert incoming cells to the next level to prevent obstruction in that region. This is verified with experimental observations showing the ability of the microdevice to effectively direct the cells away from occupied traps (Movie 1). For the purpose of cell retrieval, the flow direction is reversed (Fig. 2b) by applying a positive pressure differential across the waste outlet and cell collection point. During cell retrieval, the inverted isolation structures enable a streamline profile that minimize impediment to the cells ensuring a high percentile of retrieval. The rounded base of the crescent traps also help to minimize obstructions to the cells during retrieval to prevent external trauma which may be detrimental to the isolated cells (Chang et al. 2008).

Figure 2(c) shows the wall shear stress profile of an isolated cell in the crescent trap. Contrasting to the physiological states experienced in large arteries (1.0–7.0 Pa) (Malek et al. 1999), the estimated average wall shear stress around the isolated cells due to the flow are comparable (1.80 Pa). This indicates that the cells are likely to maintain its integrity whilst in the microdevice. Figure 3 depicts the estimated wall shear stress over a range of input pressures. The operating range of 5–15 kPa is selected for driving the flow in the microdevice so that the wall shear stress is within the range of physiological conditions.

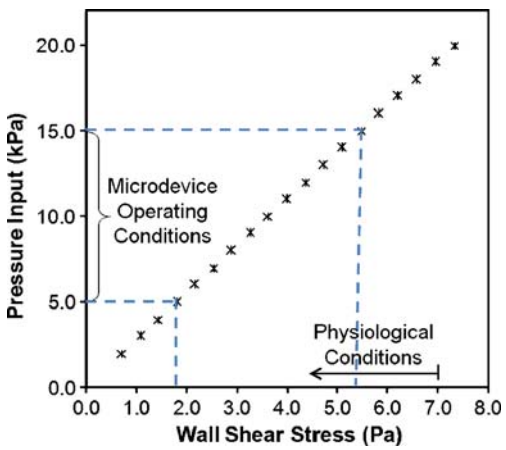

Fig. 3 Effects of input pressure on the estimated wall shear stress of an isolation cell using simulation studies

3.2 Cancer cell isolation efficiency

For characterizing the cell isolation efficiency, low concentration of cancer cells (100 cells per milliliter) spiked in 1× PBS is injected into the microdevice at various pressure differentials. Small numbers of cancer cells in the sample solution mimic the rarity of CTCs in peripheral blood. By visually counting the number of trapped and escaped cancer cells, the efficiency of cancer cell capture can be determined using equation 1.

$$\textit{Isolation Efficiency}(\%) = \frac{\textit{Trapped Cells}}{\textit{Trapped Cells} + \textit{Escaped Cells}} \times 100\% \quad (1)$$

The main factor affecting cell isolation efficiency is the pressure applied as the input condition directly alters the flow conditions in the device. Although, higher flow rates meant less sample processing time, the larger shear forces on the cells are undesirable as they can cause cell behaviour modifications due to mechanically activated signal pathways or cell death (Chang et al. 2008). In this investigation, the selected pressure differentials include 5 kPa, 10 kPa and 15 kPa which are comparable to physiological conditions. Figure 4(a) shows the successful arrest of MCF-7 breast cancer cells in the isolation structures (Movie 2). The single or doublet cells arrested in each isolation well also facilitated cell counting with ease. Using two pressure regulators connected to the sample inlet and the waste outlet, the pressure differential can be kept stable and used to maintain constant flow condition. The quantitative analysis from comparing cell isolation efficiency at various pressure settings is plotted in Fig. 4(b) for MCF-7, MDA-MB-231 and HT-29. The results favour the lower input pressure of 5 kPa to effectively isolate cancer cells with at least 80% isolation efficiency for all tested samples. The Student's t-test verifies that isolation efficiencies at 5 kPa are significantly higher ($p<0.01$) for all 3 samples than at higher pressure inputs. The reduction in efficiency as pressure differential increases can be accounted for by the dislodgement of the arrested cells due to increased hydrodynamic forces acting on these cells at higher pressure differentials. Experimental observations also indicate that smaller cancer cells are likely to be displaced after being momentarily trapped at higher pressure settings. At the pressure setting of 5 kPa, the microdevice is capable of processing sample at 0.7 ml/hr with a high isolation efficiency needed for an accurate diagnosis.

Other leading techniques to enrich cancer cells from peripheral blood have efficiency ranging from 20% to 90% (Allard et al. 2004; Balic et al. 2005; Lara et al. 2004). However, there are also numerous restrictions and complex preparation procedures. For example, there is limited purity when detecting low concentrations of CTCs (Smirnov et al. 2005) in peripheral blood and require various preparatory steps such as centrifugation, incubation and functional modifications which can be tedious and time consuming. The proposed microdevice is comparable to other leading biochemical techniques in terms of cancer cell enumeration from blood and is done without any functional modifica-

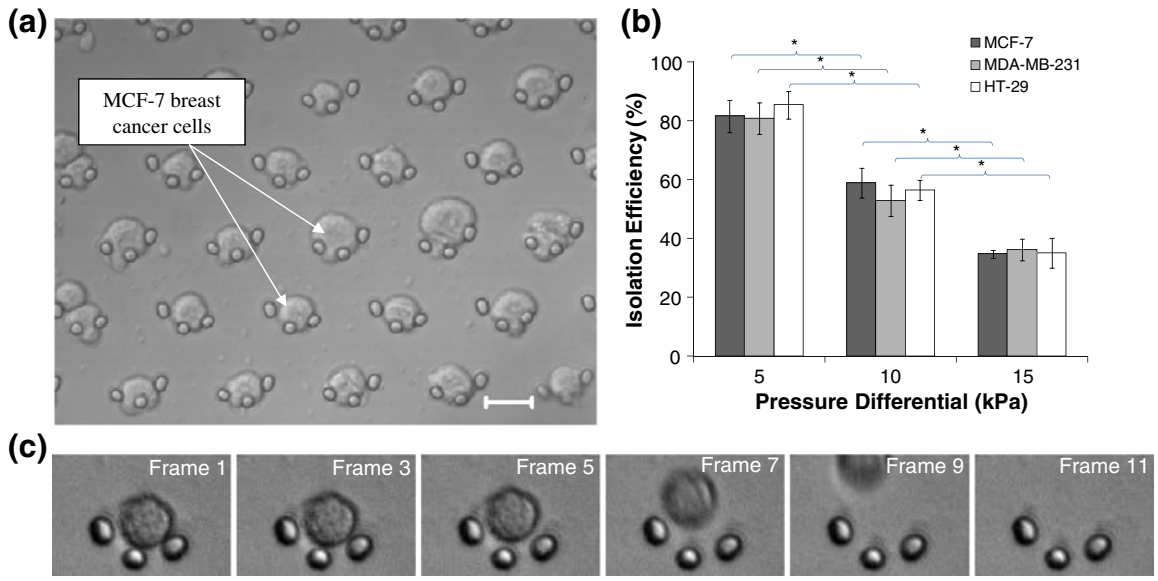

Fig. 4 Cancer cells isolation and microdevice efficiency characterization. (**a**) Overview of the cell isolation region showing mostly single cells trapped in each crescent-shaped structure. (Scale bar represents 20 μm.) (**b**) Microdevice isolation efficiency as a function of the input conditions. (A total of 70 experimental runs are tabulated and error bars indicate measurement standard deviation; * refers to $p < 0.01$ with a Student's t-test) (**c**) Time sequence images showing the retrieval an isolated MDA-MB-231 cell (Movie 3) taken at approximately 110 fps (Period of 0.1 s.)

tions. Removing isolated cells for further analysis can also be achieved with ease by altering the flow conditions to induce the cells to flow towards the cell collection point. Figure 4(c) shows the sequence of optical images depicting the typical retrieval of one of the arrested cells (Movie 3).

3.3 Cancer cell isolation purity

In order to ascertain the capture purity, cancer cells mixed with blood samples collected from healthy human volunteers (~100 cancer cells per milliliter) are diluted with 1× PBS to reduce sample viscosity and injected into the microdevice (Movie 4). To differentiate between hematologic and cancer cells, immuno-fluorescence staining of the isolated cells is carried out. It is reported that the EpCAM is over-expressed in human carcinoma (Baeuerle and Gires 2007; Osta et al. 2004) which makes this an ideal marker to identify the cancer cells. MCF-7, MDA-MB-231 and HT-29 have been reported to be positive for EpCAM (Flieger et al. 2001; Osta et al. 2004). CD45, a trans-membrane glycoprotein is expressed among hematologic cells and will be used to distinguish WBCs.

Figure 5(a) shows the immuno-fluorescence staining results of a typical experiment for the isolated cells in the microdevice. In the control experiment, cancer cells are identified using red (EpCAM positive) and blue fluorescence (DAPI positive) while hematologic cells are identified using green (CD45 positive) and blue fluorescence (DAPI positive). For the isolated cells in the microdevice, the staining protocol is repeated and Fig. 5(a) depicts that high purity can be achieved, showing the absence of WBCs (no visible green fluorescence). The purity is maintained over the entire pressure range as shown in Fig. 5(b), showing no significant difference in a Student's t-test for MCF-7, MDA-MB-231 and HT-29 cancer cells at $p<0.01$. The purity is calculated by the ratio of cancer cells to the total number of cells isolated from the blood mixture. This is also significantly higher than leading techniques which claims a separation purity of approximately 50% using biochemical means (Nagrath et al. 2007).

3.4 Conditions of isolated cells and cell retrieval

The conditions of cancer cells after isolation are of interest given that tumor cells in circulation are likely to be responsible for cancer progression. Preserving the native state of cells after isolation will help to determine their exact nature and allow a detailed study of CTC subpopulations. Retrieval of the isolated cells in the microdevice can be achieved by altering the inlet conditions with the pressure regulators. The waste reservoir is cleared first to prevent backflow of waste materials, followed by closing of the sample inlet fluidic port. The valve leading to the cell collection point is then opened and the pressure differential between the waste outlet and cell collection point quickly increased to 20 kPa. Isolated cells will then be dislodged and the recovery rate and standard deviation are determined to be (95 ± 8.0)% for MCF-7, (97 ± 2.6)% for MDA-MB-231 and (96 ± 4.4)% for HT-29. The recovery rate is calculated based on the number of cells that are dislodged to the initial number of isolated cells. The process of cell recovery is repeated for 5–8 cycles to obtain enough cell number and the retrieved cells are then reseeded to a culture flask.

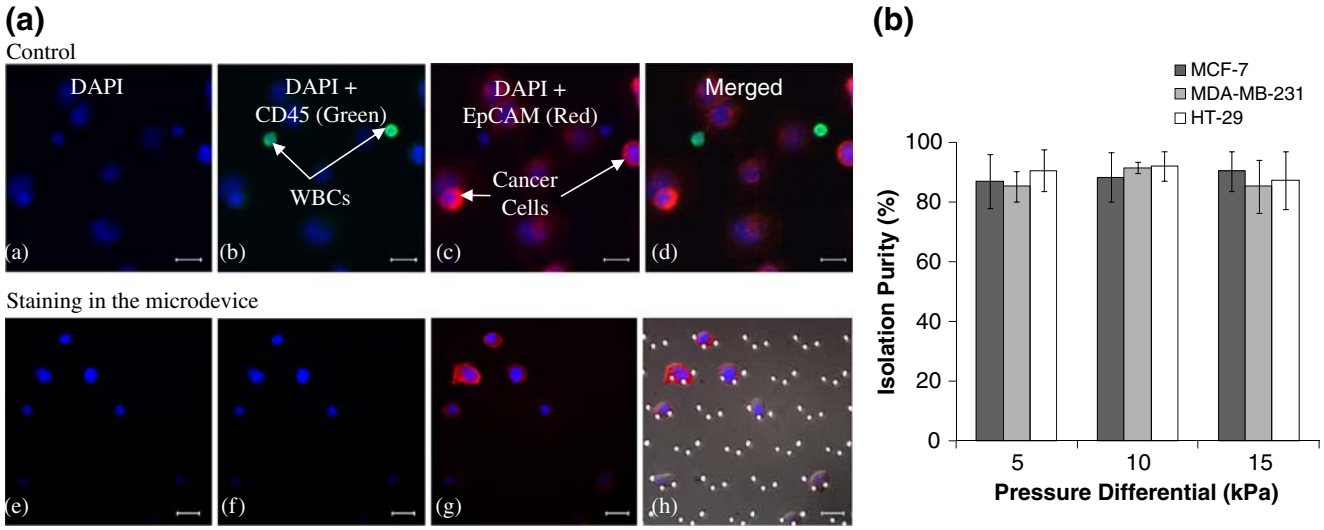

Fig. 5 Purity of cancerous cells isolation using the microdevice. (**a**) Immunofluorescence staining are performed on the control experiment (**a-d**) and isolated cells in the microdevice (**e-h**) to identify cancer cells and WBCs. EpCAM is stained with red fluorescence (cancer cells), CD45 with green fluorescence (WBCs) and nuclei materials with blue fluorescence. (Scale bar represents 20 μm.) (**b**) Purity of cancer cells isolation over various operating pressures

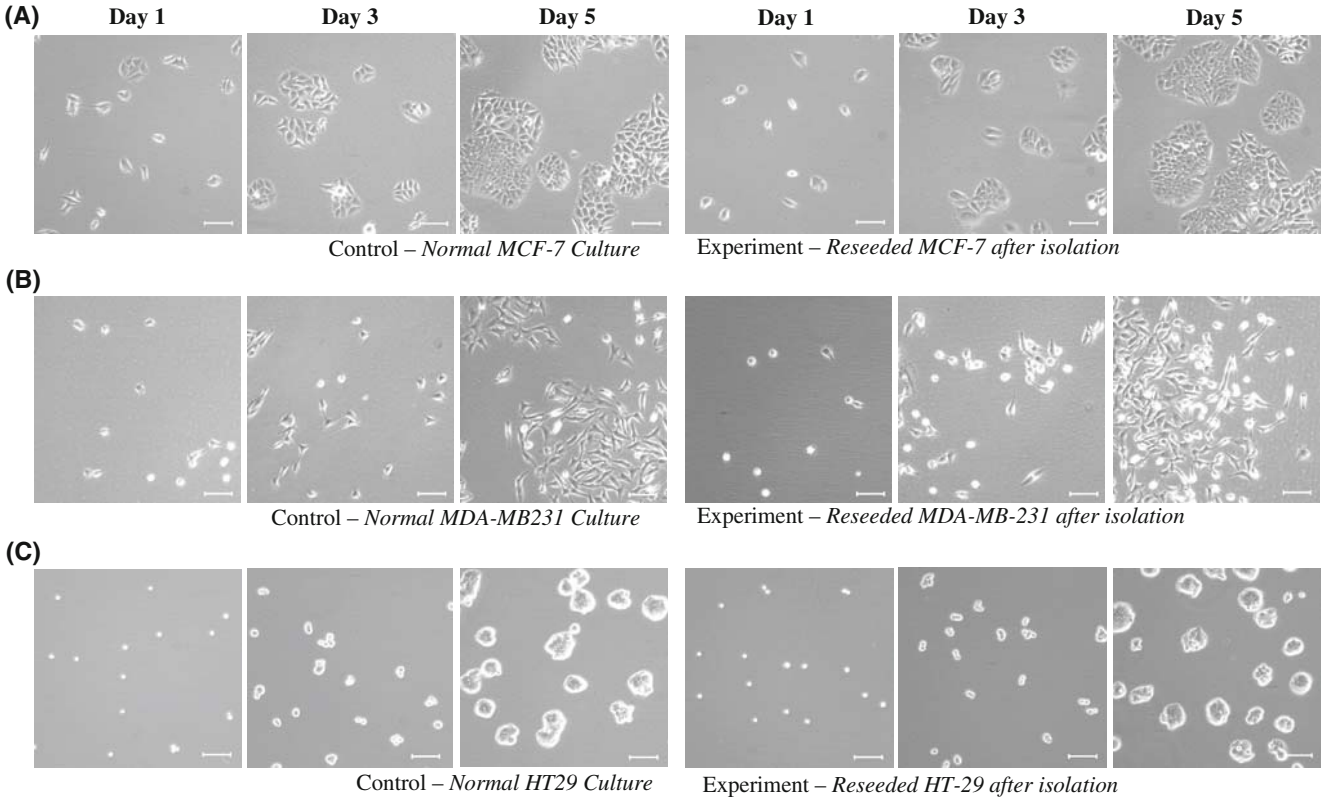

Fig. 6 Cell proliferation comparison between normal cultures (control) and retrieved cells over a period of 5 days. No observable differences in cell proliferation rate for (**a**) MCF-7 (**b**) MDA-MB-231 and (**c**) HT-29 cancer cells (Scale bar represents 100 μm.)

The proliferative rates of reseeded cells are compared to normal cultured cells which act as controls to ascertain isolated cancer cells are not affected by the microdevice. Figure 6 illustrates an overview of a 5-day culture for MCF-7, MDA-MB-231 and HT-29. Over the same time period, there are no observable differences in proliferation rate for all cell-lines when comparing against their respective normal cultures. The morphology of the retrieved cells and its control experiment are also rather similar. This uniformity in cell behaviour confirms that the retrieved cells are unaffected after isolation in the microdevice.

In clinical reports, a CTC count of 5 cancer cells per 7.5 ml of blood is significant to represent the severity of the disease (Cristofanilli et al. 2004; Nole et al. 2008). To test the effectiveness of the microdevice to function at this concentration, 1–3 cancer cells are manually picked out and added into 1 ml of PBS. The difficulties in getting reproducible cell numbers and the need for enough cells for the proliferation analysis restrict the characterization with such small cell numbers. Table 1 shows the number of isolated cancer cells with the corresponding spiked cell number. The expected cell number refers to the number of cancer cells added to 1 ml of 1× PBS and isolated cell number refers to the number of cancer cells trapped. Out of the 15 experimental runs, 11 trials achieve to isolate and recover the spiked cancer cells with a pressure input of 5 kPa which constitutes to 80% efficacy. This is in line with the results of the cancer cell isolation efficiency of the microdevice which predicts an isolation efficiency of

Table 1 Summary of the number of cancer cells isolated from low concentrations of spiked sample solutions at pressure input of 5 kPa

Cell Type	MCF-7		MDA-MB-231		HT-29	
	Expected	Isolated	Expected	Isolated	Expected	Isolated
Run 1	1	1	1	0	1	1
Run 2	2	2	1	1	1	0
Run 3	1	1	1	1	2	1
Run 4	2	1	1	1	2	2
Run 5	3	3`	2	0	1	1

approximately 80%. Overall, a total of 16 cells from all 15 experimental runs have been recovered.

4 Conclusions

Our microfluidic platform has successfully demonstrated the enumeration of cancer cells of breast and colon origin in blood samples by utilizing the stiffer and larger size characteristics of cancer cells as compared to blood constituents. This has potential in CTCs applications that can help to monitor the disease progression and treatment efficacy in contrast with biochemical techniques that are usually employed. The microdevice also achieves significant cancer cell isolation purity while preserving the integrity and state of these cells. With isolation efficiency of at least 80% for MCF-7, MDA-MB231 and HT-29, the microdevice can provide a potential useful assessment of the disease status. High cancer cell isolation purity for the microdevice will also minimize false positive results. The microdevice requires neither functional modifications nor complex enrichment procedures, simplifying operation procedures. For clinical blood tests which usually handle larger sample volumes, parallel setups using multiple microdevices simultaneously can be adopted. Flowing 5ml of sample through 3 microdevices at the same time at 5 kPa took no more than 2.5 h which is considerably shorter than most leading techniques. These unique features make our microdevice attractive for possible CTC studies and potential clinical monitoring of the disease cancer.

Acknowledgements The equipment support provided by the Global Enterprise for Micro Mechanics and Molecular Medicine (GEM4) Laboratory at the National University of Singapore is gratefully acknowledged.

References

W.J. Allard, J. Matera, M.C. Miller, M. Repollet, M.C. Connelly, C. Rao, A.G. Tibbe, J.W. Uhr, L.W. Terstappen, Clin. Cancer Res. **10**, 6897 (2004). doi:10.1158/1078-0432.CCR-04-0378

P.A. Baeuerle, O. Gires, Br. J. Cancer **96**, 417 (2007). doi:10.1038/sj.bjc.6603494

M. Balic, N. Dandachi, G. Hofmann, H. Samonigg, H. Loibner, A. Obwaller, A. van der Kooi, A.G. Tibbe, G.V. Doyle, L.W. Terstappen, T. Bauernhofer, Cytometry B Clin. Cytom. **68**, 25 (2005). doi:10.1002/cyto.b.20065

P.D. Beitsch, E. Clifford, Am. J. Surg. **180**, 446 (2000). doi:10.1016/S0002-9610(00)00518-3

G.T. Budd, M. Cristofanilli, M.J. Ellis, A. Stopeck, E. Borden, M.C. Miller, J. Matera, M. Repollet, G.V. Doyle, L.W. Terstappen, D.F. Hayes, Clin. Cancer Res. **12**, 6403 (2006). doi:10.1158/1078-0432.CCR-05-1769

S.F. Chang, C.A. Chang, D.Y. Lee, P.L. Lee, Y.M. Yeh, C.R. Yeh, C. K. Cheng, S. Chien, J.J. Chiu, Proc. Natl. Acad. Sci. USA **105**, 3927 (2008). doi:10.1073/pnas.0712353105

P.Y. Chiou, A.T. Ohta, M.C. Wu, Nature **436**, 370–372 (2005). doi:10.1038/nature03831

M. Cristofanilli, K.R. Broglio, V. Guarneri, S. Jackson, H.A. Fritsche, R. Islam, S. Dawood, J.M. Reuben, S.W. Kau, J.M. Lara, S. Krishnamurthy, N.T. Ueno, G.N. Hortobagyi, V. Valero, Clin. Breast Cancer **7**, 471 (2007). doi:10.3816/CBC.2007.n.004

M. Cristofanilli, G.T. Budd, M.J. Ellis, A. Stopeck, J. Matera, M.C. Miller, J.M. Reuben, G.V. Doyle, W.J. Allard, L.W. Terstappen, D.F. Hayes, N. Engl. J. Med. **351**, 781 (2004)

S. Dawood, K. Broglio, V. Valero, J. Reuben, B. Handy, R. Islam, S. Jackson, G.N. Hortobagyi, H. Fritsche, M. Cristofanilli, Cancer **113**, 2422 (2008). doi:10.1002/cncr.23852

D. Di Carlo, L.Y. Wu, L.P. Lee, Lab. Chip. **6**, 1445 (2006). doi:10.1039/b605937f

D. Flieger, A.S. Hoff, T. Sauerbruch, I.G. Schmidt-Wolf, Clin. Exp. Immunol. **123**, 9–14 (2001). doi:10.1046/j.1365-2249.2001.01435.x

H. Gogas, G. Kefala, D. Bafaloukos, K. Frangia, A. Polyzos, D. Pectasides, D. Tsoutsos, P. Panagiotou, J. Ioannovich, D. Loukopoulos, Br. J. Cancer **87**, 181 (2002). doi:10.1038/sj.bjc.6600419

D.S. Gray, J.L. Tan, J. Voldman, C.S. Chen, Biosens. Bioelectron. **19**, 1765–1774 (2004)

G.P. Gupta, J. Massague, Cell **127**, 679–695 (2006). doi:10.1016/j.cell.2006.11.001

D.F. Hayes, M. Cristofanilli, G.T. Budd, M.J. Ellis, A. Stopeck, M.C. Miller, J. Matera, W.J. Allard, G.V. Doyle, L.W. Terstappen, Clin. Cancer Res. **12**, 4218 (2006). doi:10.1158/1078-0432.CCR-05-2821

D.S. Hoon, Nat. Clin. Pract. Oncol. **1**, 74 (2004). doi:10.1038/ncponc0041

H.J. Kahn, A. Presta, L.Y. Yang, J. Blondal, M. Trudeau, L. Lickley, C. Holloway, D.R. McCready, D. Maclean, A. Marks, Breast Cancer Res. Treat. **86**, 237 (2004). doi:10.1023/B:BREA.0000036897.92513.72

R.T. Krivacic, A. Ladanyi, D.N. Curry, H.B. Hsieh, P. Kuhn, D.E. Bergsrud, J.F. Kepros, T. Barbera, M.Y. Ho, L.B. Chen, R.A. Lerner, R.H. Bruce, Proc. Natl. Acad. Sci. USA **101**, 10501 (2004). doi:10.1073/pnas.0404036101

O. Lara, X. Tong, M. Zborowski, J.J. Chalmers, Exp. Hematol. **32**, 891 (2004). doi:10.1016/j.exphem.2004.07.007

J.E. Losanoff, W. Zhu, W. Qin, F. Mannello, E.R. Sauter, Breast **17**, 540 (2008). doi:10.1016/j.breast.2008.04.005

A.M. Malek, S.L. Alper, S. Izumo, JAMA **282**, 2035 (1999). doi:10.1001/jama.282.21.2035

L.A. Mattano Jr., T.J. Moss, S.G. Emerson, Cancer Res. **52**, 4701 (1992)

J.C. McDonald, G.M. Whitesides, Acc. Chem. Res **35**, 491–499 (2002). doi:10.1021/ar010110q

S. Mocellin, D. Hoon, A. Ambrosi, D. Nitti, C.R. Rossi, Clin. Cancer Res. **12**, 4605 (2006). doi:10.1158/1078-0432.CCR-06-0823

H. Mohamed, L.D. McCurdy, D.H. Szarowski, S. Duva, J.N. Turner, M. Caggana, IEEE Trans. Nanobioscience **3**, 251 (2004). doi:10.1109/TNB.2004.837903

J.G. Moreno, S.M. O'Hara, S. Gross, G. Doyle, H. Fritsche, L.G. Gomella, L.W. Terstappen, Urology **58**, 386 (2001). doi:10.1016/S0090-4295(01)01191-8

S. Nagrath, L.V. Sequist, S. Maheswaran, D.W. Bell, D. Irimia, L. Ulkus, M.R. Smith, E.L. Kwak, S. Digumarthy, A. Muzikansky, P. Ryan, U.J. Balis, R.G. Tompkins, D.A. Haber, M. Toner, Nature **450**, 1235 (2007). doi:10.1038/nature06385

F. Nole, E. Munzone, L. Zorzino, I. Minchella, M. Salvatici, E. Botteri, M. Medici, E. Verri, L. Adamoli, N. Rotmensz, A. Goldhirsch, M.T. Sandri, Ann. Oncol. **19**, 891 (2007). doi:10.1093/annonc/mdm558

F. Nole, E. Munzone, L. Zorzino, I. Minchella, M. Salvatici, E. Botteri, M. Medici, E. Verri, L. Adamoli, N. Rotmensz, A.

Goldhirsch, M.T. Sandri. Ann. Oncol. **19**, 891–897 (2008) doi:10.1093/annonc/mdm558
W.A. Osta, Y. Chen, K. Mikhitarian, M. Mitas, M. Salem, Y.A. Hannun, D.J. Cole, W.E. Gillanders, Cancer Res. **64**, 5818 (2004). doi:10.1158/0008-5472.CAN-04-0754
N. Pamme, Lab Chip **7**, 1644 (2007). doi:10.1039/b712784g
K. Pantel, R.H. Brakenhoff, B. Brandt, Nat. Rev. Cancer **8**, 329 (2008). doi:10.1038/nrc2375
J.M. Reuben, S. Krishnamurthy, W. Woodward, M. Cristofanilli, Expert Opin. Med. Diagnostics **2**, 339 (2008). doi:10.1517/17530059.2.4.339
A. Rolle, R. Gunzel, U. Pachmann, B. Willen, K. Hoffken, K. Pachmann, World J. Surg. Oncol. **3**, 18 (2005). doi:10.1186/1477-7819-3-18
A. Rosenthal, J. Voldman, Biophys. J. **88**, 2193–2205 (2005). doi:10.1529/biophysj.104.049684
C.P. Schroder, M.H. Ruiters, S. de Jong, A.T. Tiebosch, J. Wesseling, R. Veenstra, J. de Vries, H.J. Hoekstra, L.F. de Leij, E.G. de Vries, Int. J. Cancer **106**, 611 (2003). doi:10.1002/ijc.11295
J.P. Shelby, J. White, K. Ganesan, P.K. Rathod, and D.T. Chiu, **100**, (2003)
D.A. Smirnov, D.R. Zweitzig, B.W. Foulk, M.C. Miller, G.V. Doyle, K.J. Pienta, N.J. Meropol, L.M. Weiner, S.J. Cohen, J.G. Moreno, M.C. Connelly, L.W. Terstappen, S.M. O'Hara, Cancer Res. **65**, 4993 (2005). doi:10.1158/0008-5472.CAN-04-4330
P.S. Steeg. Nat. Med. **12**, 895–904 (2006) doi:10.1038/nm1469
S. Steen, J. Nemunaitis, T. Fisher, J. Kuhn. Proc **21**, 127 (2008). Bayl Univ Med Cent
R. Szatanek, G. Drabik, J. Baran, P. Kolodziejczyk, J. Kulig, J. Stachura, M. Zembala. Oncol. Rep. **19**, 1055 (2008)
S.J. Tan, L. Yobas, G.Y.H. Lee, C.N. Ong, C.T. Lim, International Conference on Biocomputation, Bioinformatics, and Biomedical Technologies, 2008. BIOTECHNO '08. (2008)
S. Urtishak, R.K. Alpaugh, L.M. Weiner, R.F. Swaby, Biomarkers Med. **2**, 137 (2008). doi:10.2217/17520363.2.2.137
J. Voldman, Curr Opin Biotechnol **17**, (2006)
L. Weiss, Adv Cancer Res **54**, (1990)
L. Weiss, D.S. Dimitrov, Cell Biophys. **6**, 9 (1984)
L. Weiss, D.S. Dimitrov, J. Theor. Biol. **121**, 307 (1986)
G. Wiedswang, B. Naume, Nat. Clin. Pract. Oncol. **4**, 154 (2007)
C.S. Wong, M.T. Cheung, B.B. Ma, E. Pun Hui, A.C. Chan, C.K. Chan, K.C. Lee, W. Cheuk, M.Y. Lam, M.C. Wong, C.M. Chan, J.K. Chan, and A.T. Chan, Int. J. Surg. Pathol. **16**, (2008)
H. Yagata, S. Nakamura, M. Toi, H. Bando, S. Ohno, A. Kataoka, Int J Clin Oncol **13**, 252 (2008)
B. Yap, and R.D. Kamm, J. Appl. Physiol. **98**, (2005)
V. Zieglschmid, C. Hollmann, O. Bocher, Crit. Rev. Clin. Lab. Sci. **42**, 155 (2005)